International Journal of
Molecular Sciences

MDPI

Article

Ethyl Butyrate Synthesis Catalyzed by Lipases A and B from *Candida antarctica* Immobilized onto Magnetic Nanoparticles. Improvement of Biocatalysts' Performance under Ultrasonic Irradiation

Rodolpho R. C. Monteiro [1], Davino M. Andrade Neto [2], Pierre B. A. Fechine [2], Ada A. S. Lopes [3], Luciana R. B. Gonçalves [1], José C. S. dos Santos [3,*], Maria C. M. de Souza [3,*] and Roberto Fernandez-Lafuente [4,*]

1 Departamento de Engenharia Química, Universidade Federal do Ceará, Campus do Pici, Bloco 709, CEP 60455760, Fortaleza 60000-000, CE, Brazil; montteirorrc@gmail.com (R.R.C.M.); lrg@ufc.br (L.R.B.G.)
2 Departamento de Química Analítica e Físico-Química, Universidade Federal do Ceará, Campus do Pici, Bloco 940, CEP 60455760, Fortaleza 60000-000, CE, Brazil; davinomachado@gmail.com (D.M.A.N.); fechine@ufc.br (P.B.A.F.)
3 Instituto de Engenharias e Desenvolvimento Sustentável, Universidade da Integração Internacional da Lusofonia Afro-Brasileira, Campus das Auroras, CEP 62790970, Redenção 68550-000, CE, Brazil; ada@unilab.edu.br
4 Departamento de Biocatálisis, ICP-CSIC, Campus UAM-CSIC Cantoblanco, 28049 Madrid, Spain
* Correspondence: jcs@unilab.edu.br (J.C.S.d.S.); mariacristiane@unilab.edu.br (M.C.M.d.S.); rfl@icp.csic.es (R.F.-L.); Tel.: +55-85-3332-6109 (J.C.S.d.S. & M.C.M.d.S.); +34-915-854-941 (R.F.-L.)

Received: 31 October 2019; Accepted: 18 November 2019; Published: 19 November 2019

Abstract: The synthesis of ethyl butyrate catalyzed by lipases A (CALA) or B (CALB) from *Candida antarctica* immobilized onto magnetic nanoparticles (MNP), CALA-MNP and CALB-MNP, respectively, is hereby reported. MNPs were prepared by co-precipitation, functionalized with 3-aminopropyltriethoxysilane, activated with glutaraldehyde, and then used as support to immobilize either CALA or CALB (immobilization yield: 100 ± 1.2% and 57.6 ± 3.8%; biocatalysts activities: 198.3 ± 2.7 $U_{p\text{-NPB}}$/g and 52.9 ± 1.7 $U_{p\text{-NPB}}$/g for CALA-MNP and CALB-MNP, respectively). X-ray diffraction and Raman spectroscopy analysis indicated the production of a magnetic nanomaterial with a diameter of 13.0 nm, whereas Fourier-transform infrared spectroscopy indicated functionalization, activation and enzyme immobilization. To determine the optimum conditions for the synthesis, a four-variable Central Composite Design (CCD) (biocatalyst content, molar ratio, temperature and time) was performed. Under optimized conditions (1:1, 45 °C and 6 h), it was possible to achieve 99.2 ± 0.3% of conversion for CALA-MNP (10 mg) and 97.5 ± 0.8% for CALB-MNP (12.5 mg), which retained approximately 80% of their activity after 10 consecutive cycles of esterification. Under ultrasonic irradiation, similar conversions were achieved but at 4 h of incubation, demonstrating the efficiency of ultrasound technology in the enzymatic synthesis of esters.

Keywords: ethyl butyrate; lipase A from *Candida antarctica*; lipase B from *Candida antarctica*; magnetic nanoparticles; ultrasonic irradiation

1. Introduction

The catalysis of reactions mediated by biological catalysts is an alternative to traditional chemical catalysis [1–3]. Enzymes are biological macromolecules that reduce the occurrence of undesirable side reactions and can work under mild temperature and pressure, which minimizes the energy demand and thermal degradation of the product of interest [4,5].

In this sense, lipases (triacylglycerol hydrolases, EC 3.1.1.3) are enzymes that stand out due to the wide range of reactions that they can catalyze (e.g., hydrolysis, acidolysis, esterification, transesterification, and amination) in different media (organic solvents, ionic liquids, supercritical fluids, etc.) [6–8], with high stability and great diversity [9,10].

Lipase A (CALA) and lipase B (CALB) can be isolated from the yeast *Candida antarctica* [11,12]. CALB is the most widely used lipase, being employed in the cosmetic, pharmaceutical, food, and beverage industries [13–18]. On the other hand, CALA has not hitherto been so widely used, even though it bears several interesting features [19].

CALA (45 kDa, isoelectric point 7.5 and optimum pH 7.0) is an extremely thermostable protein (optimum temperature above 90 °C), whereas CALB has a lower stability (optimum temperature around 40 °C) [19,20]. CALA displays activity using large substrates (bulky alcohols, esters and tertiary alcohols) [21,22], and it is possible to accommodate sterically hindered substrates [23]. CALB (33 kDa, isoelectric point 6.0 and optimum pH 7.0) has a very small lid [24]. Both enzymes possess the classical serine hydrolases catalytic triad [20,25].

However, the industrial application of lipases is limited due to problems concerning their stability, recovery and reuse. A solution to these problems is their immobilization on insoluble solid supports [26]. A proper immobilization strategy, together with simplifying the enzyme reuse or use in continuous reactor, may improve enzyme stability, activity, selectivity or specificity; purify the enzyme; or decrease its inhibition [27–32].

In the case of CALB, there is an immobilized commercial preparation supplied by Novozymes, Novozym® 435, immobilized on a macroporous acrylic polymer resin (Lewatit VP OC 1600) [33]. This biocatalyst has been successfully used in diverse reactions, but it has been described to possess some limitations, like enzyme release in certain media, polymer dissolution in organic media, or the capture of hydrophilic compounds in the enzyme environment [33–39]. Thus, an alternative support may further increase the implementation of these interesting enzymes. For example, lipase immobilization on magnetic nanoparticles (MNPs) allows easy recovery of the enzyme by application of a magnetic field [2]; besides, the enzyme will be immobilized on the external area of the nanoparticle and this avoids any kind of diffusional limitation. This also raised some problems (e.g., the enzyme is exposed to all inactivating external interfaces [28]). Moreover, these supports have a high surface area, may be easily modified to introduce groups with chemical reactivity, and have a high thermal stability [40–42]. Therefore, magnetic nanoparticles have become versatile and interesting immobilization supports to achieve enzyme immobilization/stabilization via multipoint covalent attachment; aminated supports can be easily activated using glutaraldehyde [43].

Covalent attachment is a very convenient method for enzymatic immobilization [44–48]. Glutaraldehyde is a very widely used method to immobilize enzymes on primary amino functionalized supports [49–51]. The supports activated with glutaraldehyde are very versatile, due to the presence of hydrophobic, ionic and chemically reactive moieties [43,50,51]. In amino glutaraldehyde preactivated supports, the enzyme–support interactions are very strong and the leaching of the enzyme is minimized, which produces a more stable biocatalyst [47].

Short chain fatty acids are used as aroma and flavors and may be extracted from natural products, but at a very high price and low yield [52]. The industrial production of these esters employs acidic catalysts. This implies a great demand for energy and the promotion of side reactions, causing environmental problems and requires complex downstream development [53–55]. Moreover, the final products cannot be labeled as natural [56]. In contrast, enzymatic catalysis allows the production of products that can be labelled as natural and the reaction is performed under mild conditions with lower environmental impact [57]. Among these esters, ethyl butyrate is applied as an aroma and fragrance compound in beverage, food, cosmetic, and pharmaceutical industries [2,51,58].

The direct enzymatic esterification between an acid and an alcohol is called thermodynamically controlled synthesis [59]. The yields are independent from the catalysts, which only determine the feasibility of the process (e.g., the thermodynamic yields may not be reached if the catalyst is inactivated

or inhibited). The main problem of this reaction is water production. If water is captured (e.g., using molecular sieves), the yields may be shifted towards the synthesis, and also this may permit preventing the formation of an aqueous phase on the biocatalyst beads (where the water is formed). This water layer can inhibit or inactivate the enzyme [60]. This has been solved using very hydrophobic supports and also using ultrasonic irradiation to stir inside the biocatalyst and to prevent this aqueous phase formation [61–64].

Ultrasound is the use of sonic energy at frequencies >20 kHz and requires a medium to propagate [65]. The consecutive cycles of compression and rarefaction of sound waves can cause a phenomenon known as cavitation, which comprises the formation, enlargement and collapse of bubbles, which, when it occurs near the limit phase of two immiscible liquids, can provide a very efficient stirring, facilitating mass transfer; furthermore, the collapse of the bubbles causes supercritical conditions of temperature and pressure [66,67].

On the other hand, optimization of the process when some variables can co-interact is not simple using a standard optimization protocol due to the high number of experiments that this may require [68]. In this sense, the statistical methodologies of design, such as the Central Composite Design (CCD), allow the study of the covariance of the variables (independent factors) to obtain the best response (dependent factor) with a reduced number of runs [69].

Therefore, the main objective of this communication is to synthesize ethyl butyrate using lipases A or B from *Candida antarctica* immobilized onto iron magnetic nanoparticles coated with 3-aminopropyltriethoxysilane and activated with glutaraldehyde, (CALA-MNP and CALA-MNP). Fixing an acid concentration of 1.0 M, the influence of temperature, reaction time, molar ratio, and content of the biocatalyst were evaluated in the production of this flavor ester by a CCD. The thermodynamic parameters of the reactions (variations of enthalpy and entropy and Gibbs free energy) were also established as well as the operational stability of the enzymatic biocatalyst.

2. Results and Discussion

2.1. Immobilization Performance

As it is shown in Table 1, for the covalent immobilization (1 mg of protein for 1 g of support, pH 7.0, 25 mM and 25 °C), the immobilization yield was 100% for CALA-MNP and 57.6% for CALB-MNP; for both biocatalysts, a reference solution was prepared (an enzyme solution under identical conditions to those of immobilization but in absence of support) and it maintained full activity during all immobilization processes, so the immobilization yield could be calculated by the decrease of activity in the supernatant. The performance of immobilization was evaluated by recovery activity as well, presenting a value of 97.5% for CALA-MNP and 80.5% for CALB-MNP. As it is seen in Table 1, for the adsorption immobilization, both biocatalysts performed worse than the glutaraldehyde activated nanoparticles, showing that glutaraldehyde plays a significant role in enzyme immobilization.

Table 1. Immobilization parameters of CALA and CALB: immobilization yield (IY), theoretical biocatalyst activity (At_T), biocatalyst activity (At_D) and recovery activity (At_R) (1 mg of protein per 1 g of support was the loading of the supports, and the experiments were performed in 0.25 mM sodium phosphate at pH 7 and 25 °C). Further details are given in Section 3.

Biocatalyst	IY (%)	At_T (U/g)	At_D (U/g)	At_R (%)
Fe_3O_4@APTES–GLU–CALA	100 ± 1.2	203.3 ± 1.2	198.3 ± 2.7	97.5 ± 1.9
Fe_3O_4@APTES-CALA	80 ± 3.1	110.7 ± 3.1	46.2 ± 3.3	41.7 ± 3.2
Fe_3O_4@APTES–GLU–CALB	57.6 ± 3.8	65.7 ± 3.8	52.9 ± 1.7	80.5 ± 3.2
Fe_3O_4@APTES-CALB	38.2 ± 3.3	43.6 ± 3.3	31.3 ± 1.2	71.3 ± 2.2

The support used in this communication, having a high surface density of amino groups and activated with glutaraldehyde, may permit hydrophobic, anionic exchange and covalent interactions

with the enzyme [30,70]. Lipases may become immobilized onto the support first via a rapid interfacial activation, which is faster than the direct covalent attachment; however, the use of ionic strength and detergents may ensure immobilization firstly via direct covalent attachment [51].

At neutral pHs, glutaraldehyde groups are more stable than at alkaline pHs and the most reactive group in the enzyme tends to be the terminal amino group [71]. Moreover, if more enzyme nucleophile groups are exposed to the support, other covalent bonds between the enzyme and support may be established [72], enabling multipoint covalent immobilization.

2.2. Characterization of Fe_3O_4 NPs

XRD and Raman spectroscopy analysis were performed to confirm the success in the synthesis of the magnetic core of the biocatalysts, as shown in Figure 1. It was noticed by XRD analysis that the magnetic core is composed by a single structural phase, cubic inverse spinel structure *Fd3m*, which is characteristic of Fe_3O_4 and γ-Fe_2O_3 (see Figure 1A). The cubic cell lattice parameter for our sample was 8.371 (5) Å, which is an intermediate value between Fe_3O_4 and γ-Fe_2O_3, indicating a partially oxidized Fe_3O_4 NPs (8.396 Å for Fe_3O_4 and 8.346 Å for γ-Fe_2O_3) [73,74]. The crystallite size of the sample was calculated by Scherrer's equation. A diameter of 13.0 (2) nm was found, indicating the preparation of a nanoparticulate material.

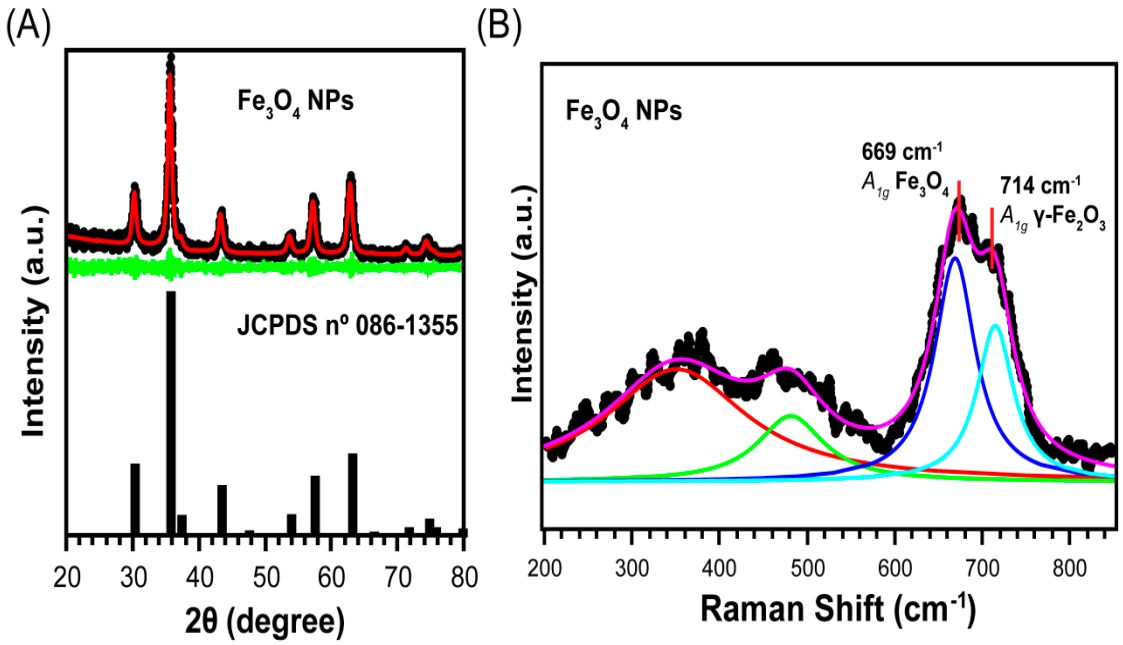

Figure 1. (**A**) XRD patterns of the Fe_3O_4 NPs synthesized herein; black dots and the red and green lines represent the measurement data, adjusted diffractogram and subtraction between the measurement data and adjusted diffractogram, respectively. (**B**) Raman spectrum of the Fe_3O_4 NPs; black dots and the pink line are the measurement data and the Lorentzian fit, respectively. Other colored lines are adjusted vibrational modes of the Fe_3O_4 NPs. Further details are given in Section 3.

Even though XRD was not conclusive in relation to the different phases of the iron oxides, Raman spectroscopy was able to differentiate Fe_3O_4 from γ-Fe_2O_3 [75]. Figure 1B shows a typical Raman spectrum for nanoparticles with broad peaks and relatively low signal-to-noise ratio. The band centered in 669 cm^{-1} can be attributed to A_{1g} phonon mode of Fe_3O_4, while a shoulder in 714 cm^{-1} corresponds to the A_{1g} mode of γ-Fe_2O_3. Additionally, the modes in 350 and 432 cm^{-1} can be assigned to T_{2g} and E_g of γ-Fe_2O_3 [76]. The presence of these aforementioned vibrational modes confirms that the magnetic core of the biocatalysts prepared herein is composed by Fe_3O_4 and γ-Fe_2O_3.

2.3. Fourier-Transform Infrared Spectroscopy (FT-IR)

Fourier-transform Infrared Spectroscopy (FT-IR) analysis of all samples was performed aiming to confirm the success of the modifications proposed in this communication. In Figure 2, the FT-IR spectra in the range of 800–1800 cm^{-1} are shown. All samples presented a set of bands in 490–770 cm^{-1} relative to the Fe–O stretching of the Fe_3O_4 MNPs, which corroborates with results of DRX and Raman spectroscopy (see Figure 1). After functionalization with APTES, a set of bands in 893, 995 and 1112 cm^{-1} were evidenced, which are attributed to Si–O–H and Si–O–Si groups of APTES [77] ((Figure 2A,B), spectrum of Fe_3O_4@APTES). Furthermore, amine groups of APTES onto the surface of Fe_3O_4 NPs can be evidenced by the vibrational mode in 1628 cm^{-1}, relative to NH_2 bending [77]. Non-covalent immobilization of CALA and CALB on the surface of Fe_3O_4@APTES can be confirmed by the appearance of the vibrational modes in 1632–1631 and 1033–1036 cm^{-1} relative to amide I and stretching of C–N, respectively ((Figure 2A,B), spectrum of Fe_3O_4@APTES-CALA and Fe_3O_4@APTES-CALB) [78]. The activation of the sample Fe_3O_4@APTES with GLU is confirmed by the presence of the bands in 1628, 1701 and 2862–2930 cm^{-1}, which are attributed to the stretching of C = N, C = O and C–H groups, respectively [79,80]. Moreover, the presence of CALB and CALA, after the covalent immobilization onto Fe_3O_4@APTES-GLU, is confirmed by the bands of amide I and II in 1637–1638 and 1537–1544 cm^{-1}, respectively [78]. Additionally, for the spectra of the samples Fe_3O_4@APTES-GLU-CALA and Fe_3O_4@APTES-GLU-CALB, it was evidenced by a diminishing/disappearance of the C = O stretching in 1701 cm^{-1} due to the reaction between the aldehyde groups of Fe_3O_4@APTES-GLU and residual amine groups of CALB and CALA. Therefore, the results of FT-IR corroborate the success of the modifications of the surface of Fe_3O_4 MNPs and preparation of the biocatalysts.

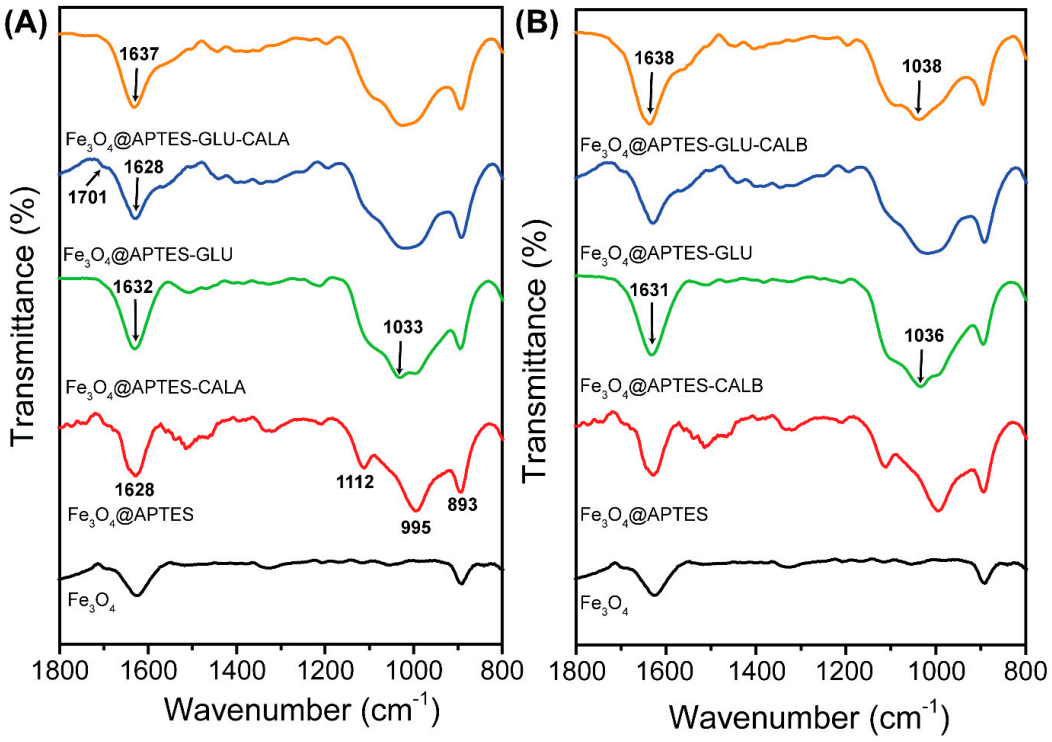

Figure 2. FT-IR spectra for the nanoparticles obtained in this communication. In each column is shown the series of spectra for (**A**) CALA and (**B**) CALB immobilization.

2.4. Model Fitting and ANOVA

In order to determine the optimal enzyme content, molar ratio, temperature, reaction time, and substrate molar ratio for the synthesis of ethyl butyrate using heptane and solvent and CALA-MNP or CALB-MNP as biocatalysts, a CCD was carried out and the results are presented in Table 2. For both

biocatalysts, the highest conversion (96.3 ± 2.1% for CALA-MNP and 92.3 ± 2.7% for CALB-MNP) was obtained for run 19 (10 mg of biocatalyst, 1:1, 45 °C and 6 h).

Table 2. Coded values and results for the CCD. Further details are given in Section 3.

Run	X_1	X_2	X_3	X_4	Conversion (%)	
					CALA-MNP	CALB-MNP
1	−1	−1	−1	−1	65.4 ± 1.4	70.5 ± 2.6
2	−1	−1	−1	1	72.3 ± 1.0	78.3 ± 2.0
3	−1	−1	1	−1	70.5 ± 0.3	63.3 ± 1.8
4	−1	−1	1	1	75.4 ± 0.4	67.9 ± 0.1
5	−1	1	−1	−1	40.0 ± 1.2	42.8 ± 0.2
6	−1	1	−1	1	35.5 ± 1.0	40.7 ± 2.0
7	−1	1	1	−1	44.2 ± 0.7	31.1 ± 3.3
8	−1	1	1	1	38.8 ± 0.2	34.7 ± 0.0
9	1	−1	−1	−1	63.8 ± 0.4	73.5 ± 1.0
10	1	−1	−1	1	76.9 ± 1.0	83.3 ± 2.7
11	1	−1	1	−1	75.8 ± 1.9	69.1 ± 1.7
12	1	−1	1	1	77.1 ± 1.7	70.0 ± 2.9
13	1	1	−1	−1	40.8 ± 0.3	43.1 ± 0.9
14	1	1	−1	1	38.6 ± 0.2	43.8 ± 1.1
15	1	1	1	−1	45.2 ± 1.4	39.8 ± 1.6
16	1	1	1	1	40.2 ± 0.2	36.6 ± 2.8
17	−1	0	0	0	77.3 ± 2.0	71.2 ± 2.5
18	1	0	0	0	84.0 ± 1.6	77.7 ± 1.4
19	0	−1	0	0	96.3 ± 2.1	92.3 ± 2.7
20	0	1	0	0	73.8 ± 2.4	74.7 ± 2.9
21	0	0	−1	0	75.4 ± 2.0	65.3 ± 2.4
22	0	0	1	0	85.6 ± 2.0	73.4 ± 2.9
23	0	0	0	−1	76.1 ± 1.2	70.0 ± 2.0
24	0	0	0	1	80.2 ± 1.5	77.4 ± 2.2
25(C)	0	0	0	0	88.1 ± 1.0	83.2 ± 1.0
26(C)	0	0	0	0	89.1 ± 0.0	83.8 ± 1.4
27(C)	0	0	0	0	89.6 ± 0.1	83.3 ± 0.1

At a confidence interval of 95%, the statistical analysis of the model was done by Fisher's statistical test for analysis of variance. For both biocatalysts, the computed F-values (91.76 for CALA-MNP and 26.22 for CALB-MNP) were highly significant ($p < 0.0001$). The model fitting was checked by the determination coefficient (R^2) and correlation coefficient (R). The determination coefficient ($R^2 = 0.99$ for CALA-MNP and $R^2 = 0.97$ for CALB-MNP) implies that sample variation of up to 95% for both biocatalysts is attributed to the independent variables and can be explained by the model. For this study, both biocatalysts presented a value of R over 0.90 ($r = 0.97$ for CALA-MNP and $r = 0.93$ for CALB-MNP), suggesting a satisfactory representation of the process and an excellent correlation between the experimental results and the theoretical values predicted by the model polynomial equation, which is given below.

$$\begin{aligned} Y_{CALA-MNP} = \; & -145.33 + 6.95X_1 - 0.35X_1^2 + 3.61X_2 - 1.06X_2^2 + 3.93X_3 + 0.04X_3^2 \\ & +37.1X_4 - 2.78X_4^2 - 0.02X_1X_2 + 0.02X_1X_3 + 0.03X_1X_4 - 0.01X_2X_3 \\ & -0.67X_2X_4 - 0.04X_3X_4 \end{aligned} \quad (1)$$

$$\begin{aligned} Y_{CALB-MNP} = \; & -119.56 + 6.43X_1 - 0.30X_1^2 - 8.34X_2 + 0.37X_2^2 + 4.87X_3 - 0.05X_3^2 \\ & +38.22X_4 - 2.08X_4^2 - 0.01X_1X_2 + 0.01X_1X_3 - 0.04X_1X_4 + 0.01X_2X_3 \\ & -0.37X_2X_4 - 0.02X_3X_4 \end{aligned} \quad (2)$$

In which, Y is the conversion for the esterification reaction; and X_1, X_2, X_3, and X_4 are the coded values of enzyme content, molar ratio, temperature, and reaction time, respectively.

For the synthesis of ethyl butyrate biocatalyzed by CALA-MNP, the optimal conditions were found to be 10 mg of biocatalyst, 1:1 (butyric acid/ethyl alcohol), obtaining a theoretical value of 100% for the conversion predicted by the model after 6 h of reaction at 45 °C and 150 rpm. For CALB-MNP, the optimal conditions were found to be 12.5 mg of the biocatalyst, 1:1 (butyric acid/ethyl alcohol), obtaining a theoretical yield of 98.3% after 6 h of incubation at 45 °C and 150× *rpm*. Under the optimized conditions, experimental validation of the proposed model was conducted. After three repetitions of the procedure by titration, the conversion obtained was 99.2 ± 0.3% (CALA-MNP) and 97.5 ± 0.8% (CALB-MNP), which shows an excellent correlation between the experimental and statistically predicted results.

In a similar study, Souza et al. (2017) evaluated the esterification of butyric acid with ethyl ethanol by CALB-MPN for the synthesis of ethyl butyrate, achieving conversions over 90% after 8 h of incubation at 25 °C and 150× *rpm* for 10 mg of CALB-MNP and 1:1 (acid/alcohol) [2]. Other authors evaluated the synthesis of ethyl butyrate biocatalyzed by lipase from *Rhizomucor miehei* immobilized onto chitosan; as a result, a conversion over 90% was achieved after 6 h of incubation at 25 °C and 150× *rpm* for 200 mg of biocatalyst and 1:1 (acid/alcohol) [81]. Therefore, the optimized operational conditions obtained in this communication for the synthesis of ethyl butyrate are in accordance with those reported in the literature; however, slightly higher conversions were achieved for both biocatalysts under study at higher temperatures.

In order to evaluate the influence of biocatalyst content, molar ratio (butyric acid/ethyl alcohol), temperature and time on the synthesis of ethyl butyrate biocatalyzed by CALA-MNP or CALB-MNP, surface response methodology were plotted, as can be seen in Figure 3.

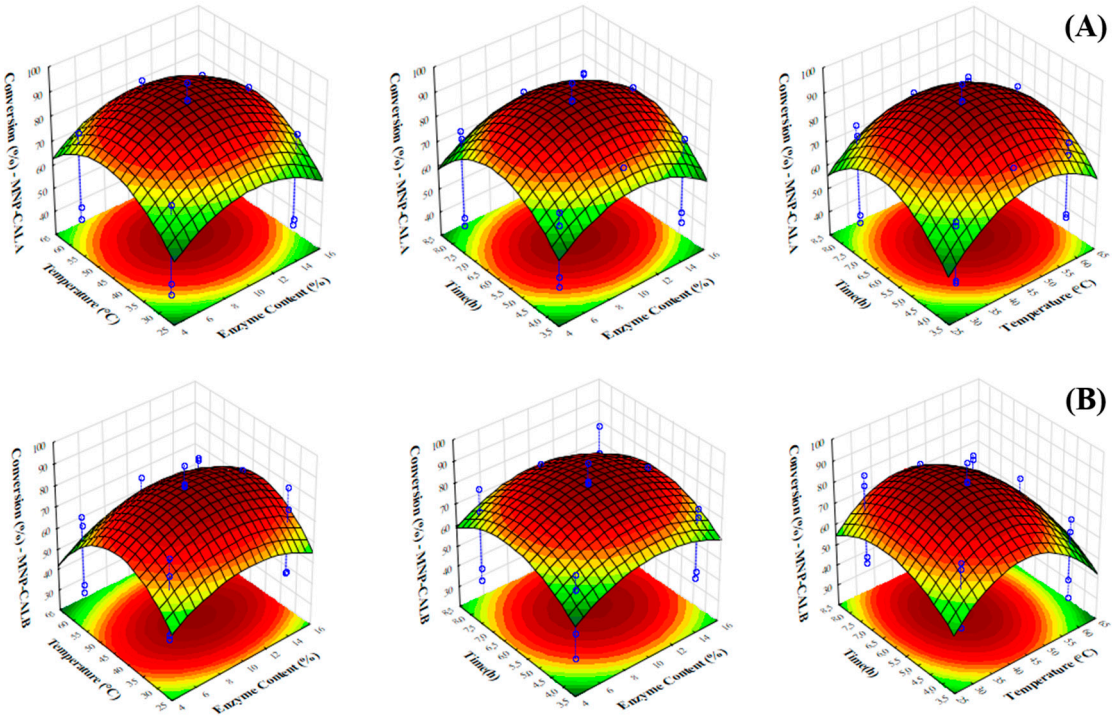

Figure 3. Fitted response surfaces. (**A**) CALA-MNP; (**B**) CALB-MNP. Reaction medium: CALA-MNP or CALB-MNP (5–15 mg), butyric acid (1.0 mol/L), ethyl alcohol 1:1–1:5 (butyric acid/ethyl alcohol), and heptane (reaction volume = 1.0 mL). The reactions were performed for 4–8 h at 30–60 °C and 150× *rpm*. Further details are given in Section 3.

For CALA-MNP, temperature was the only independent variable that positively affected the conversion, meaning that changing the level of the variable from −1 to 1 (or from 30 to 60 °C) significantly increased the response. According to Figure 3A, it can be stated that conversion increases with temperature for the studied temperature range until a certain level. Indeed, temperature is a

crucial factor for enzymatic biocatalysis, since it increases the solubility of reactants in the reaction medium, may reduce medium viscosity, and in that way, reduces mass transfer limitations; besides, it facilitates with the molecular collision interface, decreasing the energy barrier between the molecules of reactants and enabling the formation of an enzyme–substrate complex, which causes an increase in the initial rate of reaction and, therefore, causes an improvement in the conversion [82,83]. Enzymes are stable at a certain temperature range, overpassing this, the increase in temperature leads to thermal denaturation of the enzyme molecule [84].

For CALB-MNP, biocatalyst content was the independent variable that most positively affected the conversion. According to Figure 3B, it can be stated that conversion tends to increase with increasing enzyme content. Indeed, increasing the biocatalyst content may positively affect rates of reactions catalyzed by immobilized enzymes, provided that they do not aggregate forming large pellets with high diffusion limitations [83,85].

Molar ratio was the independent variable that most affected the conversion for both biocatalysts (CALA-MNP and CALB-MNP). In fact, under optimized conditions, increasing the amount of ethyl alcohol for both systems decreased the conversion by a factor of 1.3 for 1:4 (acid/alcohol). A large amount of ethanol may decrease the conversion due to its polar character, which shows hydrophilic interaction with the water layer present on the surface of the enzyme and may cause changes in the macromolecule structure with consequent inhibition and reduction of enzyme activity [86]. During the first step of esterification, ethyl alcohol at higher concentrations may promote its binding to the enzyme, decreasing the concentration of butyric acid in the vicinity of the enzyme and, therefore, reducing the reaction rate [87].

2.5. Time Course of Esterification

Once the optimal conditions for the production of ethyl butyrate catalyzed by CALA-MNP or CALB-MNP were determined by the experimental design and then validated, the conversion for the time varying from 1 to 8 h for orbital shaking and ultrasonic irradiation techniques was analyzed, as is shown in Figure 4.

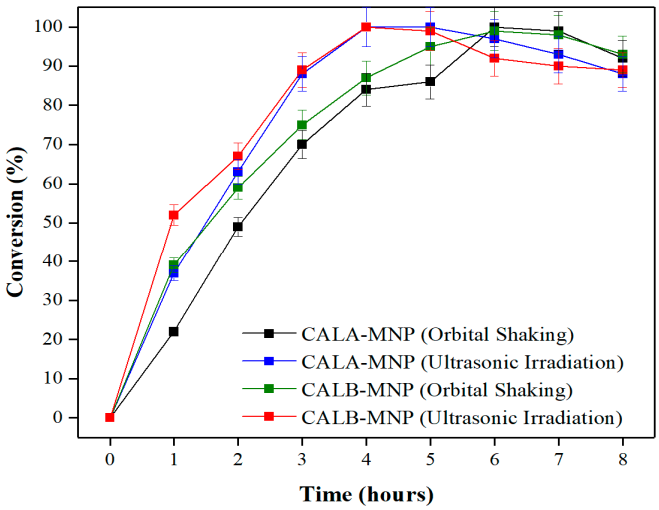

Figure 4. Esterification course for ethyl butyrate synthesis biocatalyzed by CALA-MNP or CALB-MNP under orbital shaking (150× *rpm*) or ultrasonic irradiation (37 kHz and 300 W). Reaction medium: CALA-MNP (10 mg) or CALB-MNP (12.5 mg), 1:1 (butyric acid/ethyl alcohol) and heptane (reaction volume = 1.0 mL). The reactions were performed for 1–8 h at 45 °C. Further details are given in Section 3.

As can be seen in Figure 4, for CALA-MNP, the highest conversion achieved for the orbital shaking technique was 100 ± 2.9% after 6 h of incubation. For the ultrasonic irradiation technique, the same conversion (100 ± 1.6%) was achieved after 4 h. A similar behavior was observed for CALB-MNP.

Indeed, for the orbital shaking technique, the highest conversion (99 ± 3.3%) was achieved after 6 h of incubation, whereas for the ultrasonic irradiation technique, the highest conversion (100 ± 1.2%) was achieved after 4 h.

Using an immobilized lipase, Badgujar and Bhanage (2015) synthetized benzyl butyrate, anisyl butyrate and o-cresyl butyrate by using the ultrasonic irradiation technique (33 kHz and 100 W) and obtained a conversion of 99% after 3 h of incubation at 52 °C. In the same conditions, the authors synthetized these flavor esters without using ultrasonic irradiation and obtained conversions of 57%, 55% and 43% for benzyl butyrate, anisyl butyrate and o-cresyl butyrate, respectively [86].

Therefore, ultrasonic irradiation may favor the synthesis of flavor esters catalyzed by immobilized lipases by achieving higher conversions at smaller reaction times, when compared to the traditional mechanical techniques. In fact, the ultrasonic irradiation creates supercritical conditions of temperature and pressure, besides a very efficient agitation, which facilitates mass transfer and allows the dissociation of water molecules and dissolved oxygen, creating highly reactive free radicals (-OH and -OOH) [85,88]. Nevertheless, it is known that ultrasonic cavitation may cause changes in protein conformation, affecting its catalytic activity [89]. Indeed, high frequencies and potencies can cause denaturation of enzymes, while low frequencies and potencies will not result in the desired effect [90].

For this communication, the value of frequency (37 kHz) and power (300 W) favored the enzymatic synthesis of ethyl butyrate biocatalyzed for immobilized enzymes (CALA-MNP or CALB-MNP).

2.6. Thermodynamics of the Enzymatic Esterification

By employing the van't Hoff equation (Equation (5)), the variations in enthalpy (ΔH) and entropy (ΔS) were determined from the angular and linear coefficient, respectively, of the straight line of ln K_{EQ} versus reciprocal temperature. The graphic method utilized in this communication, as it is known, is such a rough estimation to determine such thermodynamics properties; however, a more rigorous method involves quantum mechanics, which is very difficult to apply to biological systems and is not the purpose of this communication [91]. Table 3 shows the variation in enthalpy (ΔH) and entropy (ΔS) for the enzymatic synthesis of ethyl butyrate biocatalyzed by CALA-MNP or CALB-MNP under orbital shaking or ultrasonic irradiation. The regression coefficients (R^2) for all values were over 0.90.

Table 3. Variation of enthalpy and entropy for the synthesis of ethyl butyrate biocatalyzed by CALA-MNP or CALB-MNP under optimal conditions of orbital shaking (150× *rpm*) and ultrasonic irradiation (37 kHz, 300 W). Further details are given in Section 3.

	CALA-MNP		CALB-MNP	
	Orbital Shaking	**Ultrasonic Irradiation**	**Orbital Shaking**	**Ultrasonic Irradiation**
ΔH (kJ/mol)	223.1	507.8	369.9	779.1
ΔS (kJ/mol·K)	0.8	1.7	1.3	2.6

As can be seen in Table 3, for all systems, the positive values of enthalpy variation (ΔH) imply the endothermic nature of the esterification system; therefore, an increase in temperature is expected to favor product formation [92]. Indeed, for this communication, increasing the temperature has increased the K_{EQ} value, since higher temperatures intensify successful collisions of the substrates with the active site of the enzymes [93]. Similarly, for all systems, the positive values of the entropy change (ΔS) imply that the esterification system is becoming increasingly disordered as the temperature increases; besides, the formation of water molecules, as a byproduct of esterification, increases the disorder of the system [93].

For both biocatalysts under study, the variations in enthalpy and entropy were approximately twice bigger for the ultrasonic irradiation system, when compared to the orbital shaking one. The variation in enthalpy depends on the structure of the enzyme and its capacity of formation and disruption of chemical bonds [94], whereas the variation in entropy is associated with the number of molecules of the substrates with sufficient energy to react [95,96]. In fact, at 37 kHz, 300 W and for the range

of temperature under study (30 to 45 °C), the ultrasonic irradiation has favored the synthesis of ethyl butyrate biocatalyzed by immobilized lipases. Yet, for temperatures over 45 °C, the conversion decreased increasing temperature. Ultrasound irradiation at low frequencies is not able to inactivate enzymes [97], but the combined effects of ultrasound irradiation (frequency and power) and temperature (over 45 °C) may have led to the progressive inactivation of the proteins, since the conversion decreased increasing temperature.

Once the variation in enthalpy and entropy were calculated, it was possible to determine the Gibbs free energy by Equation (4), considering an interval of temperature from 303 to 333 K. Figure 5 shows the Gibbs free energy for the range of temperature under study [98].

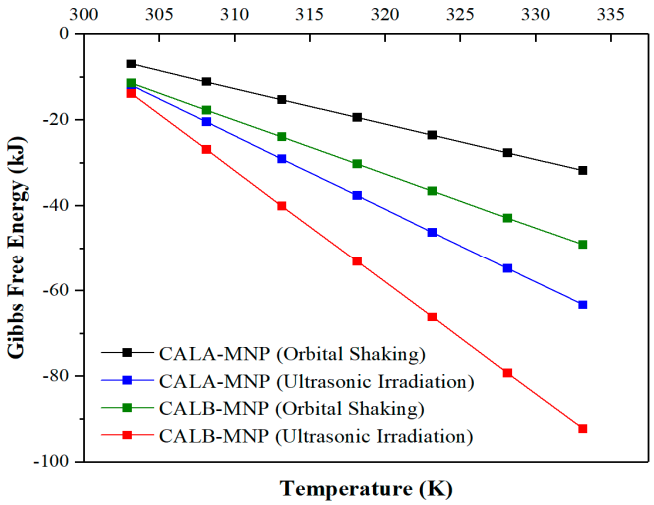

Figure 5. Gibbs free energy change for the enzymatic esterification as a function of temperature biocatalyzed by CALA-MNP or CALB-MNP under optimal conditions at orbital shaking (150× *rpm*) and ultrasonic irradiation (37 kHz, 300 W). Further details are given in Section 3.

2.7. Operational Stability

The operational stability of CALA-MNP and CALB-MNP were evaluated for the synthesis of ethyl butyrate under optimized conditions. Novozym® 435 was used for comparison purposes. To do so, consecutives cycles of esterification were performed, as is shown in Figure 6.

Enzymes have higher prices than chemical catalysts; thus, to be competitive, immobilized enzymes should be able to be reused several times, maintaining operational stability [99]. In fact, even though enzymes are very sensitive to changes in the environment, the immobilization of such biological macromolecules may promote their rigidification, which keeps the enzyme active for longer periods of time, allowing consecutive reuses [99]. As is shown in Figure 6, none of the biocatalysts have a very significant drop in activity after 10 consecutive cycles of esterification.

In order to evaluate if any chemical change happened after the reuse of the biocatalysts, FT-IR analysis of the samples Fe_3O_4@APTES-GLU-CALA and Fe_3O_4@APTES- GLU-CALB after the last cycle was performed. As is shown in Figure 7, structural changes in the spectra of the biocatalysts after reuse is not evident. All bands relative to the Fe_3O_4 core and modifications that were made remained in the spectra after reuse. Therefore, the covalent immobilization prevented any leaching of CALA or CALB from Fe_3O_4@APTES-GLU and any decrease in activity over the consecutive cycles of esterification may be related to the deactivation of the enzymes by temperature, solvents, substrate, and mechanical agitation.

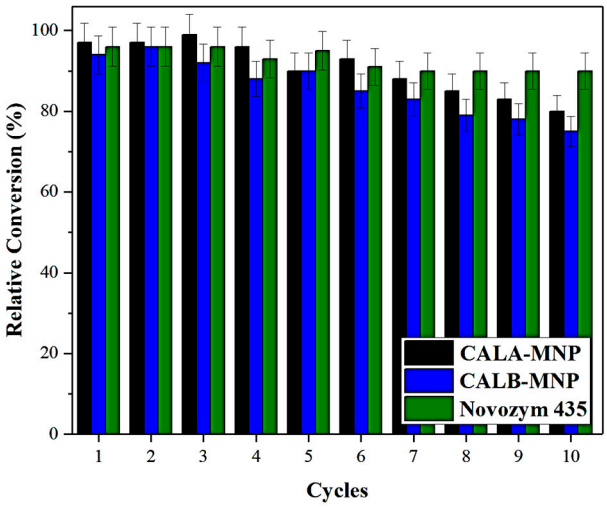

Figure 6. Operational Stability. Black column: CALA-MNP; blue column: CALB-MN; green column: Novozym®435. Reaction medium: CALA-MNP: 10 mg of biocatalyst, 1:1, 6 h of incubation at 45 °C and 150× *rpm*; CALB-MNP and Novozym® 435: 12.5 mg of biocatalyst, 1:1, 6 h of incubation at 45 °C and 150× *rpm*. Further details are given in Section 3.

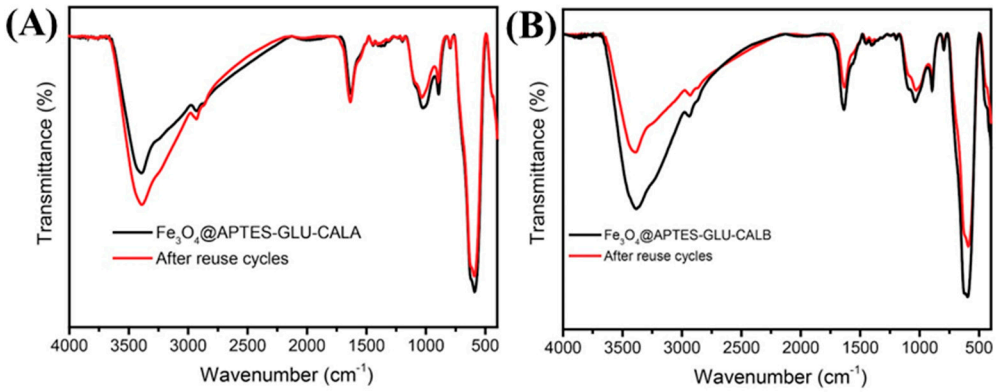

Figure 7. FT-IR spectra for CALA-MNP (**A**) and CALA-MNP (**B**) before and after 10 consecutive reuses. Further details are given in Section 3.

3. Materials and Methods

3.1. Materials

Lipases A (20.88 mg/mL) and B (7.88 mg/mL) from *Candida antartica* were kindly donated by Novozymes (Alcobendas, Spain). Lipase B from *Candida antartica* immobilized on acrylic resin (Novozym® 435), 3-aminopropyltriethoxysilane (APTES), glutaraldehyde solution grade II 25% (*w*/*v*), and *p*-nitrophenyl butyrate (*p*-NPB) were purchased from Sigma-Aldrich (Sigma-Aldrich, St Louis, MI, USA). Iron magnetic nanoparticles (Fe_3O_4) were produced by the co-precipitation method. The chemical reagents used for this synthesis were $FeCl_3.6H_2O$ (pure granulated 99%), $FeSO_4.7H_2O$ (pure granulated 99%) and 30% ammonia solution, supplied by Sigma-Aldrich (Sigma-Aldrich, St Louis, MI, USA). All reagents of analytical grade were purchased from Synth (São Paulo, Brazil) and Vetec (São Paulo, Brazil).

3.2. Methods

3.2.1. Ultrasound Equipment Setup

The equipment used was an ultrasonic bath (Unique Inc., model USC 2800A, São Paulo, Brazil). The equipment presents a capacity volume of 9.5 L with the following dimensions: 300 × 240 × 150 mm (length × width × height). Two disc transducers were placed at the bottom of the reactor. The ultrasonic frequency was 37 kHz and the total ultrasonic power 300 W. Additionally, the equipment has temperature control.

3.2.2. Synthesis of Iron Magnetic Nanoparticles (Fe_3O_4) Functionalized with 3 Aminopropyltriethoxysilane (APTES)

Firstly, 2.5 g of $FeSO_4{\cdot}7H_2O$ (9 mmol) and 4.0 g of $FeCl_3{\cdot}6H_2O$ (15 mmol) were dissolved in 30 mL of deionized water under mechanical stirring at 60 °C for 30 min. Then, 40 mL of concentrated ammonium hydroxide were added to the iron cations solution. The system remained at 60 °C under mechanical stirring for more than 30 min. Afterwards, the black nanoparticles were washed several times with deionized water and three times with ethanol.

For the functionalization with APTES, non-functionalized Fe_3O_4 NPs were dispersed in 300 mL of ethanol (95%), under room temperature, using an ultrasound bath (37 kHz and 300 W) for 1 h. Subsequently, 10 mL of APTES were added to the nanoparticle's dispersion. The system continued with sonication for more than 1 h. Finally, functionalized nanoparticles were washed four times with ethanol and dried under vacuum.

3.2.3. Activation of Fe_3O_4@APTES with Glutaraldehyde (GLU)

The amino terminal groups of Fe_3O_4@APTES were activated with glutaraldehyde (Fe_3O_4@APTES-GLU) to promote covalent attachment between the enzyme and the support, via formation of an imine bond. To do so, 250 μL of glutaraldehyde were placed in direct contact with 0.1 g of previously dried Fe_3O_4@APTES. The mixture was kept under constant stirring for 1 h at 25 °C and, after that, it was washed three times with sodium phosphate buffer solution (25 mM and pH 7.0) to remove the excess of glutaraldehyde [100].

3.2.4. Covalent Immobilization of CALA or CALB onto Fe_3O_4@APTES-GLU

Lipase A from *Candida antartica* (CALA, 20.88 mg/mL) and lipase B from *Candida antartica* (CALB, 7.88 mg/mL) were immobilized on Fe_3O_4@APTES-GLU, here named Fe_3O_4@APTES-GLU-CALA and Fe_3O_4@APTES-GLU-CALB, respectively, (CALA-MNP and CALB-MNP, respectively, for short) by covalent attachment. To do so, 0.1 mg of Fe_3O_4@APTES-GLU were suspended in 10 mL of sodium phosphate buffer solution (25 mM and pH 7.0) containing CALA or CALB (enzyme loading: 1 mg/g of support) in the presence of 0.01% Triton X-100. The system was kept under constant stirring for 2 h at 25 °C. Finally, the immobilized lipases were separated from the solution by magnetic decantation and washed with sodium phosphate buffer solution (25 mM and pH 7.0) to neutrality. The amount of enzyme immobilized on the support was determined by measuring the initial and final concentration of CALA or CALB in the supernatant of the immobilization suspension [44].

3.2.5. Adsorption Immobilization of CALA or CALB onto Fe_3O_4@APTES

Lipase A from *Candida antartica* (CALA, 20.88 mg/mL) and lipase B from *Candida antartica* (CALB, 7.88 mg/mL) were immobilized on Fe_3O_4@APTES-GLU, here named Fe_3O_4@APTES-GLU-CAL and Fe_3O_4@APTES-GLU-CALB, respectively, (CALA-MNP and CALB-MNP, respectively, for short) by adsorption. To do so, 0.1 g of Fe_3O_4@CHI-GLU were suspended in 10 mL of sodium phosphate buffer solution (25 mM and pH 7.0) containing CALA or CALB (enzyme loading: 1 mg/g of support) in the presence of 0.01% Triton X-100. The immobilization process was similar to that described in the previous section.

3.2.6. Determination of Enzymatic Activity and Protein Concentration

The activity of the soluble and immobilized enzyme was determined by the hydrolysis of *p*-NPB as a substrate; the *p*-nitrophenol concentration was quantified spectrophotometrically at 348 nm. Activity measurements were performed in sodium phosphate buffer solution (25 mM and pH 7.0) at 25 °C, from the measurement of *p*-nitrophenol released during the hydrolysis of 0.5 mM *p*-NPB (ε = 10.052 mol/cm under these conditions) [101]. To initiate the reaction, 50 µL of suspended lipase solution was added to 50 µL of *p*-NPB and 2.5 mL of the buffer solution. An international unit of activity (U) was defined as the amount of enzyme that hydrolyzes 1 µmol of *p*-NPB per minute under the conditions described above. The protein concentration was measured by the Bradford method [102], and bovine serum albumin was used as reference.

3.2.7. Immobilization Parameters

The performance of the immobilized enzyme was evaluated by the immobilization parameters described by Silva et al. [103]. In short, the immobilization yield (IY) was defined as the ratio between the activity of enzymes retained on the support (initial activity–final activity) and initial activity. The theoretical activity (At_T) was calculated using the immobilization yield (IY) and the enzyme load. The recovery activity (At_R) was determined as the ratio between the biocatalyst activity (At_B) and theoretical activity (At_T).

3.2.8. X-Ray Diffraction (XRD)

X-Ray Diffraction (XRD) profiles were collected by a X'Pert MPD X-ray powder diffractometer (PANalytical, Westborough, MA, USA) with 40 kV and 30 mA in a scanning range of 2θ = 20–80° equipped with a Co Kα tube. The diffraction patterns were obtained using Bragg-Brentano geometry in continuous mode with a speed of 0.5°/min and step size of 0.02° (2θ). The Rietveld structure refinement was used to interpret and analyze the diffraction data using the program DBWstools 2.4 [104]. The full width at half maximum (FWHM) of the instrument was calculated with the standard lanthanum hexaboride. Parameters extracted from the refinement, both the percentage of errors (15.25%) and goodness of fitting values (0.86), were found to be in agreement with those of a high-quality refinement [105]. The crystallite size of each sample was calculated using Scherrer's equation.

3.2.9. Raman Spectroscopy

Raman spectra was recorded using a LabRAM HR (HORIBA Scientific, Kyoto, Japan). The spectral excitation was performed with a laser using a 632.8 nm line, with an adjustable D1 filter with effective powers of 10.7 µW with three accumulations of 10 s. Previous to the adjustment, the spectrum was mathematically adjusted by a Savitzky–Golay filter.

3.2.10. Fourier-transform Infrared Spectroscopy (FT-IR)

The functionalized MNPs and enzyme immobilization were studied by Fourier-transform infrared spectroscopy (FT-IR). The spectra were recorded by using a Shimadzu model 8300 spectrophotometer. The samples were ground in an agate mortar and pressed into pellets of KBr. The range used was 400–4000 cm^{-1}, with a resolution of 2 cm^{-1} and 128 scans.

3.2.11. Enzymatic Esterification

The synthesis of ethyl butyrate by esterification was conducted in a reaction medium containing heptane, butyric acid (1.0 mol/L) and ethanol for molar varying from 1:1 to 1:5 (acid/alcohol), totalizing a reactional medium of 1 mL. A biocatalyst mass (CALA-MNP or CALB-MNP) of 5–15 mg was added to initiate the reaction, which was carried out under orbital shaking (150× *rpm*), at 30–60 °C for time varying from 4 to 8 h. Conversion was monitored by determining the acidity index through the Ca 5–40 AOCS method [104].

3.2.12. Central Composite Design (CCD)

In order to determine the optimal conditions for the synthesis of ethyl butyrate, a central composite design (CCD) of four variables (enzyme content, molar ratio, temperature, and reaction time) was carried out. Table 4 shows the four variables, each at three levels. The design was performed by 24 tests at factorial points and three with repetitions at the central point.

Table 4. Variables and their levels for the CCD.

Variable	Name	Coded Levels		
		−1	0	+1
X_1	Enzyme Content (mg)	5	10	15
X_2	Molar Ratio (acid/alcohol)	1:1	1:3	1:5
X_3	Temperature (°C)	30	45	60
X_4	Time (h)	4	6	8

The adjusted experimental data is shown by the proposed model in Equation (1), which considers the linear, quadratic and interaction effects among the variables, and it was used to plot response surfaces for all variables.

$$Y = \beta_0 + \sum \beta_i X_i + \sum \beta_i X_i X_j + \sum X_{ii} X_i^2 \quad (3)$$

In which, Y is the response variable; β_0 is the constant; β_i, β_{ii}, *and* β_{ij} are the coefficients for the linear, quadratic, and interaction effects, respectively; and X_i and X_j are the coded levels of variables X_i and X_j.

3.2.13. Statistical Analysis

The softwares Statistica® 10 (Statsoft, Tulsa, OK, USA) and OriginPro 2017 (OriginLab, Northampton, MA, USA) were used for the experimental design and statistical analysis for the ethyl butyrate production process. The statistical analysis of the model was performed by analysis of variance (ANOVA). The significance of the regression coefficients and the associated probabilities, p(t), were determined by Student's t-test; the second order model equation significance was determined by Fisher's F-test. The variance explained by the model is given by the determination coefficients, R^2.

3.2.14. Operational Stability

Operational stability was evaluated by consecutive reactions for the synthesis of ethyl butyrate under optimized conditions. Prior to each cycle, the biocatalysts were separated from the reaction medium by magnetization and washed three times with hexane to remove unreacted products and substrates.

3.2.15. Thermodynamic Properties

For the purpose of this study, it was considered that there was enough time for the reaction to achieve equilibrium [91]. The apparent equilibrium constant, K_{EQ}, may be obtained by Equation (4) for equimolar stoichiometry.

$$K_{EQ} = \frac{[W][E]}{[AC][AL]} = \frac{x^2}{(1-x)^2} \quad (4)$$

In which, [W], [E], [AC], and [AL] represent, respectively, the water, ester, acid, and alcohol concentration; and x represents the equilibrium conversion. The equilibrium constant dependence of temperature is given by the equation of van't Hoff (Equation (5)).

$$\ln K_{EQ} = \frac{-\Delta H}{RT} + \frac{\Delta S}{R} \quad (5)$$

In which, ΔH (J/mol), ΔS (J/mol.K), R (J/mol.K), and T (K) represent enthalpy variation, entropy variation, universal gas constant, and temperature, respectively. Once the enthalpy and entropy variation for the reaction were obtained, the Gibbs free energy was estimated by Equation (6). In which, ΔG represents the free energy of Gibbs (J/mol).

$$\Delta G = \Delta H - T\Delta S \quad (6)$$

4. Conclusions

The synthesis of ethyl butyrate biocatalyzed by lipases A or B from *Candida antarctica* immobilized onto magnetic nanoparticles (functionalized with APTES and activated with glutaraldehyde) is a promising alternative for the production of such a flavor ester, when compared to the traditional industrial processes of extraction and production using chemical catalysts, since CALA-NPM and CALB-MNP exhibit high specificity and selectivity and have the possibility of easy reuse of these biocatalysts. Besides, by the ultrasound-assisted synthesis, it was possible to achieve conversions (over 97% for both biocatalysts) similar to those achieved by orbital shaking, but at a smaller reaction time (6 h against 4 h), demonstrating the efficiency of ultrasonic irradiation for the synthesis of ethyl butyrate biocatalyzed by immobilized lipases.

Author Contributions: Conceptualization, M.C.M.d.S. and R.R.C.M.; methodology, M.C.M.d.S., R.R.C.M., D.M.A.N. and A.A.S.L.; software, R.R.C.M.; validation, R.R.C.M.; formal analysis, R.R.C.M. and D.M.A.N. investigation, R.R.C.M., D.M.A.N. and A.A.S.L.; resources, M.C.M.d.S., J.C.S.d.S., R.F.-L., P.B.A.F. and L.R.B.G.; data curation, P.B.A.F. and L.R.B.G.; writing—original draft preparation, R.R.C.M and D.M.A.N.; writing—review and editing, R.F.-L. and P.B.A.F.; visualization, M.C.M.d.S., J.C.S.d.S. and R.F.-L.; supervision, M.C.M.d.S. and J.C.S.d.S.; project administration, M.C.M.d.S. and J.C.S.d.S.; funding acquisition, M.C.M.d.S, J.C.S.d.S., L.R.B.G. and P.B.A.F.

Funding: This research was funded by Fundação Cearense de Apoio ao Desenvolvimento Científico e Tecnológico (FUNCAP), grant numbers BP3-0139-00005.01.00/18 and PNE-0112-00048.01.00/16, Conselho Nacional de Desenvolvimento Científico e Tecnológico (CNPq), grant numbers 422942/2016-2, 409058/2015-5 and 408790/2016-4, Coordenação de Aperfeiçoamento de Ensino Superior (CAPES-Finance Code 001) and MICIU, grant number CTQ2015-68951-C3-3-R.

Acknowledgments: The authors would like to thank the Brazilian research-funding agencies: Fundação Cearense de Apoio ao Desenvolvimento Científico e Tecnológico (FUNCAP), Conselho Nacional de Desenvolvimento Científico e Tecnológico (CNPq), Coordenação de Aperfeiçoamento de Ensino Superior (CAPES) and Ministerio de Economía y Competitividad and FEDER funds. In addition, the authors also acknowledge Central Analítica-UFC/CT-INFRA/MCTI-SISNANO/Pró-Equipamentos. The help and suggestions from Ángel Berenguer-Murcia (Departamento de Química Inorgánica, Universidad de Alicante) are gratefully recognized.

Conflicts of Interest: The authors declare no conflict of interest. The funders had no role in the design of the study; in the collection, analyses, or interpretation of data; in the writing of the manuscript, or in the decision to publish the results.

References

1. Monteiro, R.R.C.; Lima, P.J.M.; Pinheiro, B.B.; Freire, T.M.; Dutra, L.M.U.; Fechine, P.B.A.; Gonçalves, L.R.B.; de Souza, M.C.M.; dos Santos, J.C.S.; Fernandez-Lafuente, R. Immobilization of lipase A from *Candida antarctica* onto chitosan-coated magnetic nanoparticles. *Int. J. Mol. Sci.* **2019**, *20*, 4018. [CrossRef] [PubMed]
2. de Souza, M.C.M.; dos Santos, K.P.; Freire, R.M.; Barreto, A.C.H.; Fechine, P.B.A.; Gonçalves, L.R.B. Production of flavor esters catalyzed by lipase B from *Candida antarctica* immobilized on magnetic nanoparticles. *Braz. J. Chem. Eng.* **2017**, *34*, 681–690. [CrossRef]
3. Pinheiro, M.P.; Rios, N.S.; Fonseca, T.d.S.; Bezerra, F.d.A.; Rodríguez-Castellón, E.; Fernandez-Lafuente, R.; Carlos de Mattos, M.; dos Santos, J.C.S.; Gonçalves, L.R.B. Kinetic resolution of drug intermediates catalyzed by lipase B from *Candida antarctica* immobilized on immobead-350. *Biotechnol. Prog.* **2018**, *34*, 878–889. [CrossRef] [PubMed]

4. Arsalan, A.; Younus, H. Enzymes and nanoparticles: Modulation of enzymatic activity via nanoparticles. *Int. J. Biol. Macromol.* **2018**, *118*, 1833–1847. [CrossRef] [PubMed]
5. Hasan, F.; Shah, A.A.; Hameed, A. Industrial applications of microbial lipases. *Enzyme Microb. Technol.* **2006**, *39*, 235–251. [CrossRef]
6. Elgharbawy, A.A.; Riyadi, F.A.; Alam, M.Z.; Moniruzzaman, M. Ionic liquids as a potential solvent for lipase-catalysed reactions: A review. *J. Mol. Liq.* **2018**, *251*, 150–166. [CrossRef]
7. Ghanem, A.; Aboul-Enein, H.Y. Lipase-mediated chiral resolution of racemates in organic solvents. *Tetrahedron Asymmetry* **2004**, *15*, 3331–3351. [CrossRef]
8. Kumar, A.; Dhar, K.; Kanwar, S.S.; Arora, P.K. Lipase catalysis in organic solvents: Advantages and applications. *Biol. Proced. Online* **2016**, *18*, 2. [CrossRef]
9. dos Santos, J.C.S.; Rueda, N.; Sanchez, A.; Villalonga, R.; Gonçalves, L.R.B.; Fernandez-Lafuente, R. Versatility of divinylsulfone supports permits the tuning of CALB properties during its immobilization. *RSC Adv.* **2015**, *5*, 35801–35810. [CrossRef]
10. Wiseman, A.; Wiseman, A. Handbook of enzyme biotechnology. In *Ellis Horwood Series in Biochemistry and Biotechnology Incorporating Molecular Biology*, 3rd ed.; Ellis Horwood: New York, NY, USA, 1995.
11. Høegh, I.; Patkar, S.; Halkier, T.; Hansen, M.T. Two lipases from *Candida antarctica*: Cloning and expression in *Aspergillus oryzae*. *Can. J. Bot.* **1995**, *73*, 869–875. [CrossRef]
12. Nielsen, T.B.; Ishii, M.; Kirk, O. Lipases A and B from the yeast *Candida antarctica*. In *Biotechnological Applications of Cold-Adapted Organisms*; Margesin, R., Schinner, F., Eds.; Springer: Berlin/Heidelberg, Germany, 1999; pp. 49–61.
13. Lutz, S. Engineering lipase B from *Candida antarctica*. *Tetrahedron Asymmetry* **2004**, *15*, 2743–2748. [CrossRef]
14. McCabe, R.W.; Rodger, A.; Taylor, A. A study of the secondary structure of *Candida antarctica* lipase B using synchrotron radiation circular dichroism measurements. *Enzyme Microb. Technol.* **2005**, *36*, 70–74. [CrossRef]
15. Rodrigues, D.S.; Mendes, A.A.; Adriano, W.S.; Gonçalves, L.R.B.; Giordano, R.L.C. Multipoint covalent immobilization of microbial lipase on chitosan and agarose activated by different methods. *J. Mol. Catal. B Enzym.* **2008**, *51*, 100–109. [CrossRef]
16. Kapoor, M.; Gupta, M.N. Lipase promiscuity and its biochemical applications. *Process Biochem.* **2012**, *47*, 555–569. [CrossRef]
17. Sharma, R.; Chisti, Y.; Banerjee, U.C. Production, purification, characterization, and applications of lipases. *Biotechnol. Adv.* **2001**, *19*, 627–662. [CrossRef]
18. Jaeger, K.-E.; Eggert, T. Lipases for biotechnology. *Curr. Opin. Biotechnol.* **2002**, *13*, 390–397. [CrossRef]
19. Kirk, O.; Christensen, M.W. Lipases from *Candida a antarctica*: Unique Biocatalysts from a Unique Origin. *Org. Process Res. Dev.* **2002**, *6*, 446–451. [CrossRef]
20. Kumar, R.; Kumar, V.; Mathur, D.; Kumar, R.; Kumar, A.; Prasad, A.K. Biocatalyst CAL-B catalyzed synthesis of modified nucleosides: An overview. *Synth. Commun.* **2019**, *49*, 1659–1678. [CrossRef]
21. Domínguez de María, P.; Carboni-Oerlemans, C.; Tuin, B.; Bargeman, G.; van der Meer, A.; van Gemert, R. Biotechnological applications of *Candida antarctica* lipase A: State-of-the-art. *J. Mol. Catal. B Enzym.* **2005**, *37*, 36–46. [CrossRef]
22. Hari Krishna, S.; Persson, M.; Bornscheuer, U.T. Enantioselective transesterification of a tertiary alcohol by lipase A from *Candida antarctica*. *Tetrahedron Asymmetry* **2002**, *13*, 2693–2696. [CrossRef]
23. Sandstrom, A.G.; Wikmark, Y.; Engstrom, K.; Nyhlen, J.; Backvall, J.-E. Combinatorial reshaping of the *Candida antarctica* lipase A substrate pocket for enantioselectivity using an extremely condensed library. *Proc. Natl. Acad. Sci. USA* **2012**, *109*, 78–83. [CrossRef] [PubMed]
24. Lima, R.N.; dos Anjos, C.S.; Orozco, E.V.M.; Porto, A.L.M. Versatility of *Candida antarctica* lipase in the amide bond formation applied in organic synthesis and biotechnological processes. *Mol. Catal.* **2019**, *466*, 75–105. [CrossRef]
25. Ericsson, D.J.; Kasrayan, A.; Johansson, P.; Bergfors, T.; Sandström, A.G.; Bäckvall, J.-E.; Mowbray, S.L. X-ray structure of *Candida antarctica* lipase A shows a novel lid structure and a likely mode of interfacial activation. *J. Mol. Biol.* **2008**, *376*, 109–119. [CrossRef] [PubMed]
26. Rodrigues, R.C.; Virgen-Ortíz, J.J.; dos Santos, J.C.S.; Berenguer-Murcia, Á.; Alcantara, A.R.; Barbosa, O.; Ortiz, C.; Fernandez-Lafuente, R. Immobilization of lipases on hydrophobic supports: Immobilization mechanism, advantages, problems, and solutions. *Biotechnol. Adv.* **2019**, *37*, 746–770. [CrossRef]

27. Brady, D.; Jordaan, J. Advances in enzyme immobilisation. *Biotechnol. Lett.* **2009**, *31*, 1639–1650. [CrossRef] [PubMed]
28. Garcia-Galan, C.; Berenguer-Murcia, Á.; Fernandez-Lafuente, R.; Rodrigues, R.C. Potential of different enzyme immobilization strategies to improve enzyme performance. *Adv. Synth. Catal.* **2011**, *353*, 2885–2904. [CrossRef]
29. Homaei, A.A.; Sariri, R.; Vianello, F.; Stevanato, R. Enzyme immobilization: An update. *J. Chem. Biol.* **2013**, *6*, 185–205. [CrossRef] [PubMed]
30. Mateo, C.; Palomo, J.M.; Fernandez-Lorente, G.; Guisan, J.M.; Fernandez-Lafuente, R. Improvement of enzyme activity, stability and selectivity via immobilization techniques. *Enzyme Microb. Technol.* **2007**, *40*, 1451–1463. [CrossRef]
31. Rodrigues, R.C.; Ortiz, C.; Berenguer-Murcia, Á.; Torres, R.; Fernández-Lafuente, R. Modifying enzyme activity and selectivity by immobilization. *Chem Soc Rev* **2013**, *42*, 6290–6307. [CrossRef]
32. Sheldon, R.A. Enzyme immobilization: The quest for optimum performance. *Adv. Synth. Catal.* **2007**, *349*, 1289–1307. [CrossRef]
33. Rueda, N.; dos Santos, J.C.S.; Torres, R.; Ortiz, C.; Barbosa, O.; Fernandez-Lafuente, R. Improved performance of lipases immobilized on heterofunctional octyl-glyoxyl agarose beads. *RSC Adv.* **2015**, *5*, 11212–11222. [CrossRef]
34. Garcia-Galan, C.; Barbosa, O.; Hernandez, K.; Santos, J.; Rodrigues, R.; Fernandez-Lafuente, R. Evaluation of styrene-divinylbenzene beads as a support to immobilize lipases. *Molecules* **2014**, *19*, 7629–7645. [CrossRef] [PubMed]
35. Graebin, N.G.; Martins, A.B.; Lorenzoni, A.S.G.; Garcia-Galan, C.; Fernandez-Lafuente, R.; Ayub, M.A.Z.; Rodrigues, R.C. Immobilization of lipase B from *Candida antarctica* on porous styrene-divinylbenzene beads improves butyl acetate synthesis. *Biotechnol. Prog.* **2012**, *28*, 406–412. [CrossRef] [PubMed]
36. José, C.; Toledo, M.V.; Nicolás, P.; Lasalle, V.; Ferreira, M.L.; Briand, L.E. Influence of the nature of the support on the catalytic performance of CALB: Experimental and theoretical evidence. *Catal. Sci. Technol.* **2018**, *8*, 3513–3526. [CrossRef]
37. Marty, A.; Dossat, V.; Condoret, J.-S. Continuous operation of lipase-catalyzed reactions in nonaqueous solvents: Influence of the production of hydrophilic compounds. *Biotechnol. Bioeng.* **1997**, *56*, 232–237. [CrossRef]
38. Ortiz, C.; Ferreira, M.L.; Barbosa, O.; dos Santos, J.C.S.; Rodrigues, R.C.; Berenguer-Murcia, Á.; Briand, L.E.; Fernandez-Lafuente, R. Novozym 435: The "perfect" lipase immobilized biocatalyst? *Catal. Sci. Technol.* **2019**, *9*, 2380–2420. [CrossRef]
39. Séverac, E.; Galy, O.; Turon, F.; Pantel, C.A.; Condoret, J.-S.; Monsan, P.; Marty, A. Selection of CalB immobilization method to be used in continuous oil transesterification: Analysis of the economical impact. *Enzyme Microb. Technol.* **2011**, *48*, 61–70. [CrossRef]
40. Galvão, W.S.; Neto, D.M.A.; Freire, R.M.; Fechine, P.B.A. Super-paramagnetic nanoparticles with spinel structure: A review of synthesis and biomedical applications. *Solid State Phenom.* **2015**, *241*, 139–176. [CrossRef]
41. Lei, L.; Bai, Y.; Li, Y.; Yi, L.; Yang, Y.; Xia, C. Study on immobilization of lipase onto magnetic microspheres with epoxy groups. *J. Magn. Magn. Mater.* **2009**, *321*, 252–258. [CrossRef]
42. Li, X.; Zhu, H.; Feng, J.; Zhang, J.; Deng, X.; Zhou, B.; Zhang, H.; Xue, D.; Li, F.; Mellors, N.J.; et al. One-pot polylol synthesis of graphene decorated with size- and density-tunable Fe_3O_4 nanoparticles for porcine pancreatic lipase immobilization. *Carbon* **2013**, *60*, 488–497. [CrossRef]
43. Barbosa, O.; Ortiz, C.; Berenguer-Murcia, Á.; Torres, R.; Rodrigues, R.C.; Fernandez-Lafuente, R. Glutaraldehyde in bio-catalysts design: A useful crosslinker and a versatile tool in enzyme immobilization. *RSC Adv.* **2014**, *4*, 1583–1600. [CrossRef]
44. Bezerra, R.M.; Neto, D.M.A.; Galvão, W.S.; Rios, N.S.; Carvalho, A.C.L.d.M.; Correa, M.A.; Bohn, F.; Fernandez-Lafuente, R.; Fechine, P.B.A.; de Mattos, M.C.; et al. Design of a lipase-nano particle biocatalysts and its use in the kinetic resolution of medicament precursors. *Biochem. Eng. J.* **2017**, *125*, 104–115. [CrossRef]
45. Reis, C.; Sousa, E.; Serpa, J.; Oliveira, R.; Oliveira, R.; Santos, J. Design of immobilized enzyme biocatalysts: Drawbacks and opportunities. *Quím. Nova* **2019**, *42*, 768–783. [CrossRef]

46. Bonazza, H.L.; Manzo, R.M.; dos Santos, J.C.S.; Mammarella, E.J. Operational and thermal stability analysis of *Thermomyces lanuginosus* lipase covalently immobilized onto modified chitosan supports. *Appl. Biochem. Biotechnol.* **2018**, *184*, 182–196. [CrossRef]
47. Rios, N.S.; Pinheiro, M.P.; dos Santos, J.C.S.; de S. Fonseca, T.; Lima, L.D.; de Mattos, M.C.; Freire, D.M.G.; da Silva, I.J.; Rodríguez-Aguado, E.; Gonçalves, L.R.B. Strategies of covalent immobilization of a recombinant *Candida antarctica* lipase B on pore-expanded SBA-15 and its application in the kinetic resolution of (R,S)-Phenylethyl acetate. *J. Mol. Catal. B Enzym.* **2016**, *133*, 246–258. [CrossRef]
48. Rueda, N.; dos Santos, J.C.S.; Torres, R.; Barbosa, O.; Ortiz, C.; Fernandez-Lafuente, R. Reactivation of lipases by the unfolding and refolding of covalently immobilized biocatalysts. *RSC Adv.* **2015**, *5*, 55588–55594. [CrossRef]
49. Mohamad, N.R.; Marzuki, N.H.C.; Buang, N.A.; Huyop, F.; Wahab, R.A. An overview of technologies for immobilization of enzymes and surface analysis techniques for immobilized enzymes. *Biotechnol. Biotechnol. Equip.* **2015**, *29*, 205–220. [CrossRef]
50. dos Santos, J.C.S.; Barbosa, O.; Ortiz, C.; Berenguer-Murcia, A.; Rodrigues, R.C.; Fernandez-Lafuente, R. Importance of the Support Properties for Immobilization or Purification of Enzymes. *ChemCatChem* **2015**, *7*, 2413–2432. [CrossRef]
51. Barbosa, O.; Torres, R.; Ortiz, C.; Fernandez-Lafuente, R. Versatility of glutaraldehyde to immobilize lipases: Effect of the immobilization protocol on the properties of lipase B from Candida antarctica. *Process Biochem.* **2012**, *47*, 1220–1227. [CrossRef]
52. Gumel, A.M.; Annuar, M.S.M. *Thermomyces lanuginosus* lipase-catalyzed synthesis of natural flavor esters in a continuous flow microreactor. *3 Biotech* **2016**, *6*, 24. [CrossRef]
53. Kiss, M.A.; Sefanovits-Bányai, É.; Tóth, Á.; Boross, L. Extractive synthesis of ethyl-oleate using alginate gel co-entrapped yeast cells and lipase enzyme. *Eng. Life Sci.* **2004**, *4*, 460–464. [CrossRef]
54. Gao, W.; Wu, K.; Chen, L.; Fan, H.; Zhao, Z.; Gao, B.; Wang, H.; Wei, D. A novel esterase from a marine mud metagenomic library for biocatalytic synthesis of short-chain flavor esters. *Microb. Cell Factories* **2016**, *15*. [CrossRef] [PubMed]
55. Mohamad, N.; Buang, N.A.; Mahat, N.A.; Jamalis, J.; Huyop, F.; Aboul-Enein, H.Y.; Wahab, R.A. Simple adsorption of *Candida rugosa* lipase onto multi-walled carbon nanotubes for sustainable production of the flavor ester geranyl propionate. *J. Ind. Eng. Chem.* **2015**, *32*, 99–108. [CrossRef]
56. Silva, N.C.A.; Miranda, J.S.; Bolina, I.C.A.; Silva, W.C.; Hirata, D.B.; de Castro, H.F.; Mendes, A.A. Immobilization of porcine pancreatic lipase on poly-hydroxybutyrate particles for the production of ethyl esters from macaw palm oils and pineapple flavor. *Biochem. Eng. J.* **2014**, *82*, 139–149. [CrossRef]
57. Zdarta, J.; Norman, M.; Smułek, W.; Moszyński, D.; Kaczorek, E.; Stelling, A.; Ehrlich, H.; Jesionowski, T. Spongin-based scaffolds from *Hippospongia communis* demosponge as an effective support for lipase immobilization. *Catalysts* **2017**, *7*, 147. [CrossRef]
58. Zaak, H.; Fernandez-Lopez, L.; Otero, C.; Sassi, M.; Fernandez-Lafuente, R. Improved stability of immobilized lipases via modification with polyethylenimine and glutaraldehyde. *Enzyme Microb. Technol.* **2017**, *106*, 67–74. [CrossRef]
59. Kasche, V. Mechanism and yields in enzyme catalysed equilibrium and kinetically controlled synthesis of β-lactam antibiotics, peptides and other condensation products. *Enzyme Microb. Technol.* **1986**, *8*, 4–16. [CrossRef]
60. Roby, M.H.H. Synthesis and characterization of phenolic lipids. In *Phenolic Compounds-Natural Sources, Importance and Applications*; Soto-Hernández, M., Palma-Tenango, M., Garcia-Mateos, M.d.R., Eds.; InTech: London, UK, 2017; pp. 89–116.
61. Fallavena, L.P.; Antunes, F.H.F.; Alves, J.S.; Paludo, N.; Ayub, M.A.Z.; Fernandez-Lafuente, R.; Rodrigues, R.C. Ultrasound technology and molecular sieves improve the thermodynamically controlled esterification of butyric acid mediated by immobilized lipase from *Rhizomucor miehei*. *RSC Adv.* **2014**, *4*, 8675. [CrossRef]
62. Alves, J.; Garcia-Galan, C.; Schein, M.; Silva, A.; Barbosa, O.; Ayub, M.; Fernandez-Lafuente, R.; Rodrigues, R. Combined effects of ultrasound and immobilization protocol on butyl acetate synthesis catalyzed by CALB. *Molecules* **2014**, *19*, 9562–9576. [CrossRef]
63. Wang, Y.; Pan, Y.; Zhang, Z.; Sun, R.; Fang, X.; Yu, D. Combination use of ultrasound irradiation and ionic liquid in enzymatic isomerization of glucose to fructose. *Process Biochem.* **2012**, *47*, 976–982. [CrossRef]

64. Chatel, G.; MacFarlane, D.R. Ionic liquids and ultrasound in combination: Synergies and challenges. *Chem. Soc. Rev.* **2014**, *43*, 8132–8149. [CrossRef] [PubMed]
65. Huang, C.; Miao, M.; Jiang, B.; Cui, S.W.; Jia, X.; Zhang, T. Polysaccharides modification through green technology: Role of ultrasonication towards improving physicochemical properties of (1–3)(1-6)-α-d-glucans. *Food Hydrocoll.* **2015**, *50*, 166–173. [CrossRef]
66. Bansode, S.R.; Rathod, V.K. Ultrasound assisted lipase catalysed synthesis of isoamyl butyrate. *Process Biochem.* **2014**, *49*, 1297–1303. [CrossRef]
67. Pang, Y.L.; Abdullah, A.Z.; Bhatia, S. Review on sonochemical methods in the presence of catalysts and chemical additives for treatment of organic pollutants in wastewater. *Desalination* **2011**, *277*, 1–14. [CrossRef]
68. Patience, G.S.; Bérard, A. Experimental Planning. In *Experimental Methods and Instrumentation for Chemical Engineers*; Elsevier: New York, NY, USA, 2018; pp. 65–106.
69. Getachew, A.T.; Chun, B.-S. Optimization of coffee oil flavor encapsulation using response surface methodology. *LWT Food Sci. Technol.* **2016**, *70*, 126–134. [CrossRef]
70. Liu, D.-M.; Chen, J.; Shi, Y.-P. An online immobilized α-glucosidase microreactor for enzyme kinetics and inhibition assays. *RSC Adv.* **2015**, *5*, 56841–56847. [CrossRef]
71. Barbosa, O.; Torres, R.; Ortiz, C.; Berenguer-Murcia, Á.; Rodrigues, R.C.; Fernandez-Lafuente, R. Heterofunctional supports in enzyme immobilization: From traditional immobilization protocols to opportunities in tuning enzyme properties. *Biomacromolecules* **2013**, *14*, 2433–2462. [CrossRef]
72. Bolivar, J.M.; Mateo, C.; Godoy, C.; Pessela, B.C.C.; Rodrigues, D.S.; Giordano, R.L.C.; Fernandez-Lafuente, R.; Guisan, J.M. The co-operative effect of physical and covalent protein adsorption on heterofunctional supports. *Process Biochem.* **2009**, *44*, 757–763. [CrossRef]
73. Daou, T.J.; Pourroy, G.; Bégin-Colin, S.; Grenèche, J.M.; Ulhaq-Bouillet, C.; Legaré, P.; Bernhardt, P.; Leuvrey, C.; Rogez, G. Hydrothermal synthesis of monodisperse magnetite nanoparticles. *Chem. Mater.* **2006**, *18*, 4399–4404. [CrossRef]
74. Baaziz, W.; Pichon, B.P.; Fleutot, S.; Liu, Y.; Lefevre, C.; Greneche, J.-M.; Toumi, M.; Mhiri, T.; Begin-Colin, S. Magnetic iron oxide nanoparticles: Reproducible tuning of the size and nanosized-dependent composition, defects, and spin canting. *J. Phys. Chem. C* **2014**, *118*, 3795–3810. [CrossRef]
75. Jubb, A.M.; Allen, H.C. Vibrational spectroscopic characterization of hematite, maghemite, and magnetite thin films produced by vapor deposition. *ACS Appl. Mater. Interfaces* **2010**, *2*, 2804–2812. [CrossRef]
76. Kolen'ko, Y.V.; Bañobre-López, M.; Rodríguez-Abreu, C.; Carbó-Argibay, E.; Sailsman, A.; Piñeiro-Redondo, Y.; Cerqueira, M.F.; Petrovykh, D.Y.; Kovnir, K.; Lebedev, O.I.; et al. Large-Scale Synthesis of Colloidal Fe_3O_4 Nanoparticles Exhibiting High Heating Efficiency in Magnetic Hyperthermia. *J. Phys. Chem. C* **2014**, *118*, 8691–8701. [CrossRef]
77. Feng, B.; Hong, R.Y.; Wang, L.S.; Guo, L.; Li, H.Z.; Ding, J.; Zheng, Y.; Wei, D.G. Synthesis of Fe_3O_4/APTES/PEG diacid functionalized magnetic nanoparticles for MR imaging. *Colloids Surf. Physicochem. Eng. Asp.* **2008**, *328*, 52–59. [CrossRef]
78. Andrade, L.H.; Rebelo, L.P.; Netto, C.G.C.M.; Toma, H.E. Kinetic resolution of a drug precursor by *Burkholderia cepacia* lipase immobilized by different methodologies on superparamagnetic nanoparticles. *J. Mol. Catal. B Enzym.* **2010**, *66*, 55–62. [CrossRef]
79. Azami, M.; Rabiee, M.; Moztarzadeh, F. Glutaraldehyde crosslinked gelatin/hydroxyapatite nanocomposite scaffold, engineered via compound techniques. *Polym. Compos.* **2010**, *31*, 2112–2120. [CrossRef]
80. Esmaeilnejad-Ahranjani, P.; Kazemeini, M.; Singh, G.; Arpanaei, A. Amine-functionalized magnetic nanocomposite particles for efficient immobilization of lipase: Effects of functional molecule size on properties of the immobilized lipase. *RSC Adv.* **2015**, *5*, 33313–33327. [CrossRef]
81. de Oliveira, U.M.F.; Lima de Matos, L.J.B.; de Souza, M.C.M.; Pinheiro, B.B.; dos Santos, J.C.S.; Gonçalves, L.R.B. Efficient biotechnological synthesis of flavor esters using a low-cost biocatalyst with immobilized *Rhizomucor miehei* lipase. *Mol. Biol. Rep.* **2019**, *46*, 597–608. [CrossRef]
82. Manan, F.M.A.; Rahman, I.N.A.; Marzuki, N.H.C.; Mahat, N.A.; Huyop, F.; Wahab, R.A. Statistical modelling of eugenol benzoate synthesis using *Rhizomucor miehei* lipase reinforced nanobioconjugates. *Process Biochem.* **2016**, *51*, 249–262. [CrossRef]
83. Ozyilmaz, G.; Gezer, E. Production of aroma esters by immobilized *Candida rugosa* and porcine pancreatic lipase into calcium alginate gel. *J. Mol. Catal. B Enzym.* **2010**, *64*, 140–145. [CrossRef]

84. Foresti, M.L.; Ferreira, M.L. Chitosan-immobilized lipases for the catalysis of fatty acid esterifications. *Enzyme Microb. Technol.* **2007**, *40*, 769–777. [CrossRef]
85. Wang, D.; Yan, L.; Ma, X.; Wang, W.; Zou, M.; Zhong, J.; Ding, T.; Ye, X.; Liu, D. Ultrasound promotes enzymatic reactions by acting on different targets: Enzymes, substrates and enzymatic reaction systems. *Int. J. Biol. Macromol.* **2018**, *119*, 453–461. [CrossRef] [PubMed]
86. Badgujar, K.C.; Bhanage, B.M. The combine use of ultrasound and lipase immobilized on co-polymer matrix for efficient biocatalytic application studies. *J. Mol. Catal. B Enzym.* **2015**, *122*, 255–264. [CrossRef]
87. Pires-Cabral, P.; da Fonseca, M.M.R.; Ferreira-Dias, S. Synthesis of ethyl butyrate in organic media catalyzed by *Candida rugosa* lipase immobilized in polyurethane foams: A kinetic study. *Biochem. Eng. J.* **2009**, *43*, 327–332. [CrossRef]
88. Pokhrel, N.; Vabbina, P.K.; Pala, N. Sonochemistry: Science and Engineering. *Ultrason. Sonochem.* **2016**, *29*, 104–128. [CrossRef] [PubMed]
89. O'Donnell, C.P.; Tiwari, B.K.; Bourke, P.; Cullen, P.J. Effect of ultrasonic processing on food enzymes of industrial importance. *Trends Food Sci. Technol.* **2010**, *21*, 358–367. [CrossRef]
90. Bansode, S.R.; Rathod, V.K. An investigation of lipase catalysed sonochemical synthesis: A review. *Ultrason. Sonochem.* **2017**, *38*, 503–529. [CrossRef]
91. Zhang, D.-H.; Li, C.; Zhi, G.-Y. Kinetic and thermodynamic investigation of enzymatic l-ascorbyl acetate synthesis. *J. Biotechnol.* **2013**, *168*, 416–420. [CrossRef] [PubMed]
92. Segel, I.H. *Enzyme Kinetics: Behavior and Analysis of Rapid Equilibrium and Steady State Enzyme Systems*; Wiley Classics Library, Ed.; Wiley: New York, NY, USA, 1993.
93. Razak, N.N.A.; Annuar, M.S.M. Enzymatic synthesis of flavonoid ester: Elucidation of its kinetic mechanism and equilibrium thermodynamic behavior. *Ind. Eng. Chem. Res.* **2015**, *54*, 5604–5612. [CrossRef]
94. Zhou, Z.; Shao, H.; Han, X.; Wang, K.; Gong, C.; Yang, X. The extraction efficiency enhancement of polyphenols from *Ulmus pumila L.* barks by trienzyme-assisted extraction. *Ind. Crops Prod.* **2017**, *97*, 401–408. [CrossRef]
95. Rojas, M.L.; Trevilin, J.H.; Funcia, E.d.S.; Gut, J.A.W.; Augusto, P.E.D. Using ultrasound technology for the inactivation and thermal sensitization of peroxidase in green coconut water. *Ultrason. Sonochem.* **2017**, *36*, 173–181. [CrossRef]
96. Dalagnol, L.M.G.; Silveira, V.C.C.; da Silva, H.B.; Manfroi, V.; Rodrigues, R.C. Improvement of pectinase, xylanase and cellulase activities by ultrasound: Effects on enzymes and substrates, kinetics and thermodynamic parameters. *Process Biochem.* **2017**, *61*, 80–87. [CrossRef]
97. Martins, A.B.; Schein, M.F.; Friedrich, J.L.R.; Fernandez-Lafuente, R.; Ayub, M.A.Z.; Rodrigues, R.C. Ultrasound-assisted butyl acetate synthesis catalyzed by Novozym 435: Enhanced activity and operational stability. *Ultrason. Sonochem.* **2013**, *20*, 1155–1160. [CrossRef] [PubMed]
98. Blanco, A.; Blanco, G. Elements of Thermodynamics and Biochemical Kinetics. In *Medical Biochemistry*; Elsevier: New York, NY, USA, 2017; pp. 141–152.
99. Zaak, H.; Peirce, S.; de Albuquerque, T.; Sassi, M.; Fernandez-Lafuente, R. Exploiting the versatility of aminated supports activated with glutaraldehyde to immobilize β-galactosidase from *aspergillus oryzae*. *Catalysts* **2017**, *7*, 250. [CrossRef]
100. Xie, W.; Ma, N. Immobilized Lipase on Fe_3O_4 Nanoparticles as Biocatalyst for Biodiesel Production. *Energy Fuels* **2009**, *23*, 1347–1353. [CrossRef]
101. de Souza, T.C.; de S. Fonseca, T.; da Costa, J.A.; Rocha, M.V.P.; de Mattos, M.C.; Fernandez-Lafuente, R.; Gonçalves, L.R.B.; dos Santos, J.C.S. Cashew apple bagasse as a support for the immobilization of lipase B from *Candida antarctica*: Application to the chemoenzymatic production of (R)-Indanol. *J. Mol. Catal. B Enzym.* **2016**, *130*, 58–69. [CrossRef]
102. Bradford, M.M. A rapid and sensitive method for the quantitation of microgram quantities of protein utilizing the principle of protein-dye binding. *Anal. Biochem.* **1976**, *72*, 248–254. [CrossRef]
103. Silva, J.A.; Macedo, G.P.; Rodrigues, D.S.; Giordano, R.L.C.; Gonçalves, L.R.B. Immobilization of *Candida antarctica* lipase B by covalent attachment on chitosan-based hydrogels using different support activation strategies. *Biochem. Eng. J.* **2012**, *60*, 16–24. [CrossRef]

104. Bleicher, L.; Sasaki, J.M.; Paiva Santos, C.O. Development of a graphical interface for the Rietveld refinement program *DBWS*. *J. Appl. Crystallogr.* **2000**, *33*, 1189. [CrossRef]
105. Freire, R.M.; Ribeiro, T.S.; Vasconcelos, I.F.; Denardin, J.C.; Barros, E.B.; Mele, G.; Carbone, L.; Mazzetto, S.E.; Fechine, P.B.A. $MZnFe_2O_4$ (M = Ni, Mn) cubic superparamagnetic nanoparticles obtained by hydrothermal synthesis. *J. Nanoparticle Res.* **2013**, *15*. [CrossRef]